BIOCHEMISTRY
including biophysical chemistry & molecular biology

Article

pubs.acs.org/biochemistry

Biosynthetic Assembly of the *Bacteroides fragilis* Capsular Polysaccharide A Precursor Bactoprenyl Diphosphate-Linked Acetamido-4-amino-6-deoxygalactopyranose

Anahita Z. Mostafavi and Jerry M. Troutman*

Department of Chemistry, University of North Carolina at Charlotte, 9201 University City Boulevard, Charlotte, North Carolina 28223-0001, United States

Supporting Information

ABSTRACT: The sugar capsule capsular polysaccharide A (CPSA), which coats the surface of the mammalian symbiont *Bacteroides fragilis*, is a key mediator of mammalian immune system development. In addition, this sugar polymer has shown therapeutic potential in animal models of multiple sclerosis and other autoimmune disorders. The structure of the CPSA polymer includes a rare stereoconfiguration sugar acetamido-4-amino-6-deoxygalactopyranose (AADGal) that we propose is the first sugar linked to a bactoprenyl diphosphate scaffold in the production of CPSA. In this report, we have utilized a heterologous system to reconstitute bactoprenyl diphosphate-linked AADGal production. Construction of this system included a previously reported *Campylobacter jejuni* dehydratase, PglF, coupled to a *B. fragilis*-encoded aminotransferase (WcfR) and initiating hexose-1-phosphate transferase (WcfS). The function of the aminotransferase was confirmed by capillary electrophoresis and a novel high-performance liquid chromatography (HPLC) method. Production of the rare uridine diphosphate (UDP)-AADGal was confirmed through a series of one- and two-dimensional nuclear magnetic resonance experiments and high-resolution mass spectrometry. A spectroscopically unique analogue of bactoprenyl phosphate was utilized to characterize the transfer reaction catalyzed by WcfS and allowed HPLC-based isolation of the isoprenoid-linked sugar product. Importantly, the entire heterologous system was utilized in a single-pot reaction to biosynthesize the bactoprenyl-linked sugar. This work provides the first critical step in the in vitro reconstitution of CPSA biosynthesis.

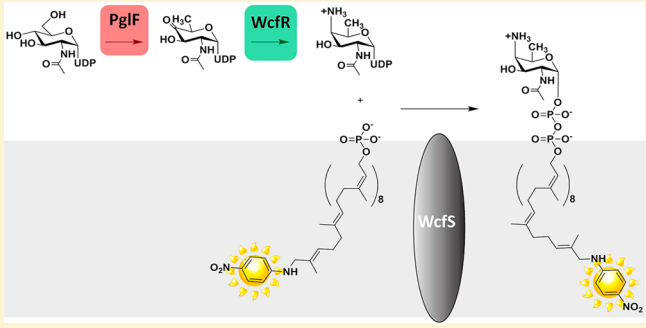

The gut microbiota plays a central role in human health, and a strong association has been noted between altered bacterial populations and disease.[1−3] Interestingly, sequenced genomes of the human microbiome are significantly enriched in metabolic enzymes involved in the metabolism of host or host diet glycans.[4] The hosts of these populations benefit through extraction of nutrients from the end products of bacterial fermentation.[2,4] The symbiont *Bacteroides fragilis* reflects this commensal relationship between host and microbe in the relatively large number of genes involved in polysaccharide metabolism.[4] The polysaccharides produced on the surface of *B. fragilis*, in particular, the capsule capsular polysaccharide A (CPSA) shown in Figure 1, have been shown to be a molecular link in the activation of $CD4^+$ T cell expression, and the early development of gut-associated lymphoid tissue.[5−8] Surprisingly, this polysaccharide has also been shown to have protective effects on autoimmune disorder models such as antibiotic-induced experimental encephalomyelitis, which is a key animal model for multiple sclerosis.[5]

The role of CPSA in human health and the potential therapeutic value of this polymer have prompted interest in its preparation as a therapeutic. Fascinating chemical synthetic work has produced CPSA, and synthesis of the tetrasaccharide repeating unit was achieved in a procedure with more than 20 steps in which the four sugars making up the unit were chemically synthesized and then linked.[9,10] However, it has been shown that at least seven or eight repeat units covalently linked are required for some of the protective effects associated with CPSA.[11] Alternatively, and more typically, CPSA has been isolated from the surface of large cultures of *B. fragilis* through a multistep isolation procedure, as eight different polysaccharides can be produced on the surface of *B. fragilis* at any time during its life cycle.[8,12] Unfortunately, bacteria may not produce consistent levels of polysaccharide materials on their surface with the exact composition from one preparation to another. Altogether, an alternative route to producing pure consistent CPSA would be of great significance to the medical community.

In this report, we have taken a biosynthetic approach to the production of the first sugar precursor in the assembly of CPSA. The gene locus responsible for polymer production by *B. fragilis* has been elucidated.[13] The function of each gene in this locus has been proposed according to the similarity of

Received: January 31, 2013
Revised: March 2, 2013
Published: March 4, 2013

dx.doi.org/10.1021/bi400126w | *Biochemistry* 2013, 52, 1939−1949

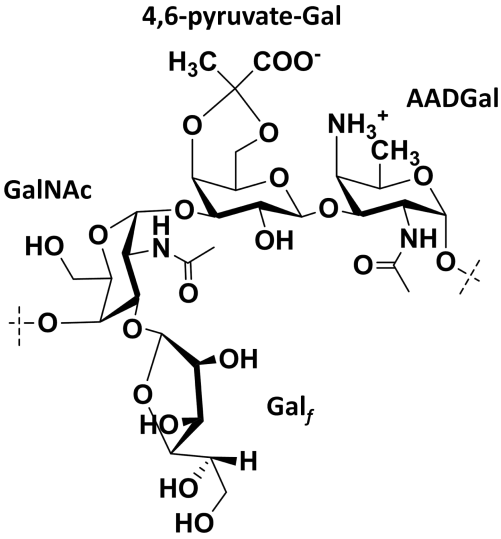

Figure 1. Capsular polysaccharide A repeat unit. The CPSA repeat unit consists of an acetamido-4-amino-6-deoxygalactopyranose (AADGal), 4,6-pyruvate galactose (4,6-pyr-Gal), *N*-acetylgalactosamine (GalNAc), and a galactofuranose (Gal$_f$) sugar. Dotted lines represent AADGal−GalNAc polymer linkage points.

translated gene sequences to known proteins and similar biosynthetic systems.[13−17] The identity of the genes present in this locus suggests that the most likely route for assembling the complex bacterial polysaccharide is a Wzy-dependent pathway in which repeat unit oligosaccharides are assembled one sugar at a time on the cytosolic face of the bacterial inner membrane.[18−22] The assembly of these oligosaccharides is thought to take place on the C55 isoprenoid bactoprenol, which acts as a hydrophobic scaffold anchoring the polymer to the membrane. It is expected that the first sugar linked to bactoprenyl phosphate, as shown in Scheme 1, is acetamido-4-amino-6-deoxygalactopyranose (AADGal).[12] On the basis of homologous systems in other organisms, a dehydratase, an aminotransferase, and an initiating hexose-1-phosphate transferase are necessary to manufacture this 4-amino sugar and link it to the bactoprenyl scaffold.[12,15,17] Within the *B. fragilis* genome CPSA biosynthesis locus are a predicted aminotransferase gene, *wcfR*, and an initiating hexose-1-phosphate transferase gene, *wcfS*, but no dehydratase.[13] However, a gene encoding a potential dehydratase has been identified elsewhere in the *B. fragilis* genome, and other organisms produce similar genes that could be used for in vitro biosynthesis of the oligosaccharide.[12,15,17]

While the genes required for CPSA biosynthesis have been suggested, there is no biochemical evidence that identifies what genes are responsible for each step of production. There are also no closely related homologues (>60% similar) of the predicted aminotransferase, WcfR, or predicted initiating hexose-1-phosphate transferase, WcfS, that have been isolated and characterized biochemically. Importantly, it has been noted that functional assignment of genes based on homology alone has been considerably problematic in numerous systems.[23,24] In this report, we have isolated, expressed, and biochemically characterized the proteins associated with the first steps in CPSA biosynthesis.

MATERIALS AND METHODS

General. UDP-[^{3}H]GlcNAc was purchased from American Radiolabeled Chemicals. Uridine-containing species were quantified by UV absorbance on a Spectramax M5 cuvette and plate reader at 260 nm using an extinction coefficient of 10000 M^{-1} cm^{-1}. *p*-Nitroaniline-containing species were quantified at 395 nm using an extinction coefficient of 9500 M^{-1} cm^{-1}. All general reagents and solvents were purchased from Sigma-Aldrich, VWR, or Fisher unless stated otherwise. Custom desalted primers were purchased from Invitrogen. Sequencing was performed by the Massachusetts Institute of Technology (MIT) Sequencing Facility. All vectors were purchased from Novagen. All high-performance liquid chromatography (HPLC) was performed on an Agilent 1100 system equipped with a diode array detector and Gilson fraction collector. Capillary electrophoresis (CE) was performed on a Beckman-Coulter P/ACE system equipped with a diode array detector, and data were collected using 32 Karat software. Thin layer chromatography (TLC) was performed on K6f nonfluorescent plates (Whatman), and plate radiolabel detection was performed on a Bioscan AR-2000 imaging scanner. Nuclear magnetic resonance (NMR) spectroscopy was performed on a 500 MHz Jeol instrument for ^{1}H NMR and

Scheme 1. Proposed Route to the Biosynthesis of Bactoprenyl Diphospho-AADGal[a]

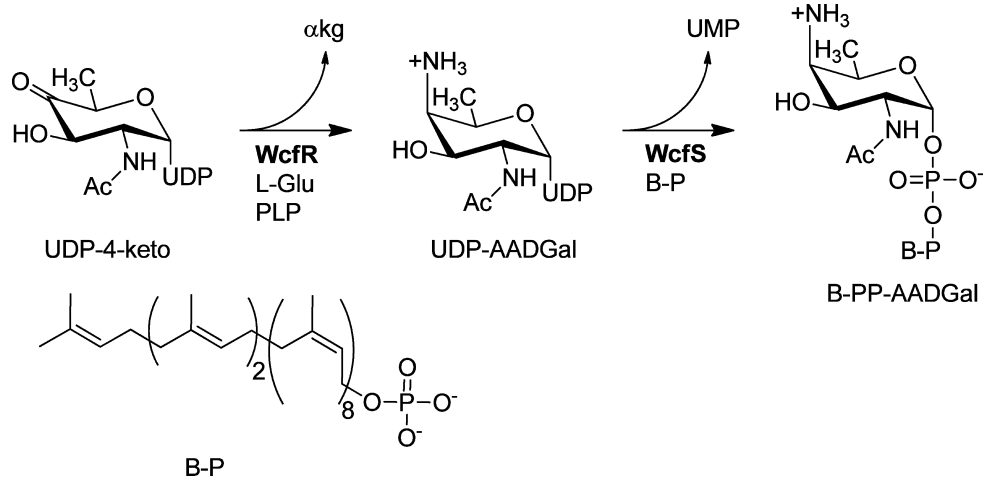

[a] αkg is α-ketoglutarate, and B-P is bactoprenyl phosphate.

dx.doi.org/10.1021/bi400126w | *Biochemistry* 2013, 52, 1939−1949

two-dimensional NMR and a 300 MHz spectrometer for ^{31}P NMR. Low-resolution electrospray ionization mass spectrometry (ESI-MS) analysis was performed in negative ion mode on a Thermo Electron Finnigan LTQ ESI-MS apparatus with injection volumes of 200 μL and concentrations ranging from 50 to 300 μM. High-resolution mass spectrometry (HR-MS) was performed at the David H. Murdock Research Institute (DHMRI) Metabolomics Laboratory by direct injection coupled to quadrapole time-of-flight MS operating in the negative mode. Isoprenoid dissolved in 20% *n*-propanol in 25 mM ammonium bicarbonate buffer at 0.1 g/L was given to the DHMRI, and UDP-AADGal was supplied at a similar concentration in 25 mM ammonium bicarbonate buffer.

Cloning. Polymerase chain reaction (PCR) amplifications of *wcfR* and *wcfS* genes were performed using *B. fragilis* genomic DNA (ATCC 25285) and oligonucleotide primers specific to each gene (Table 1 of the Supporting Information), according to the manufacturer's instructions (Promega GoTaq PCR core system 1 Kit). PCR amplifications were isolated (Promega wizard SV Gel and PCR Clean-Up System) and then digested with restriction enzymes as indicated below at 37 °C for 4 h. Insert and specified vector digests were separated by gel electrophoresis on a 1% agarose gel. The digested inserts and plasmids were extracted (Qiagen QIAquick gel extraction kit) from the gel, and inserts were ligated into corresponding plasmids overnight at 4 °C (Promega T4 DNA ligase kit). Ligated plasmids were transformed into chemically competent DH5α *Escherichia coli* cells and were plated on Luria-Bertani (LB) agar-kanamycin plates. Plasmids were isolated using a Fermentas GeneJET Plasmid Miniprep Kit and sequenced.

The *wcfR* gene was amplified with a 5′-BamHI site and 3′-XhoI site and inserted into a pET-24a vector encoding an N-terminal T7 tag and a C-terminal hexahistidine tag.

The *wcfS* gene was amplified with a 5′-NdeI site and 3′-XhoI site and inserted into a pET-24a vector encoding a C-terminal hexahistidine tag.

Expression of WcfS and WcfR by Autoinduction. Plasmids encoding WcfS and WcfR were transformed into chemically competent BL-21(DE3) RIL (Agilent) *E. coli* cells and expressed using autoinduction as described by Studier[25] with slight modification. Overnight starter cultures were prepared with frozen protein expressing glycerol stocks of cells, and 3 mL was used to inoculate 1 L of LB broth containing kanamycin, 400 mg of glucose, 1 g of lactose, 4 mL of M buffer (0.625 M Na_2HPO_4, 0.625 M KH_2PO_4, 1.25 M NH_4Cl, and 0.125 M Na_2SO_4), and 2 mL of 1 M $MgSO_4$. The WcfR- and WcfS-expressing cells were incubated at 37 °C until an optical density between 0.6 and 0.8 was reached, and the temperature was reduced to 16 °C.

Purification of WcfR. After overnight incubation, WcfR-expressing cells were harvested by centrifugation at 5000*g* and 4 °C for 30 min. The cell pellets were resuspended in 30 mL of lysis buffer [50 mM Tris-HCl (pH 8) and 200 mM NaCl] and lysed on ice via sonication (Fisher Scientific model 500 sonic dismembranator) at 25% power for 2 min with a pulse of 1 s on and 1 s off. Lysed cells were spun at 150000*g* on an ultracentrifuge (Beckman) at 4 °C for 75 min. The supernatant was passed through a 2 mL Ni-NTA Agarose (PerfectoPro, 5 Prime inc.) column. The column was washed with 4 × 3 column volumes of wash buffer [50 mM Tris-HCl (pH 8), 200 mM NaCl, and 50 mM imidazole]. The protein was eluted off the column with 6 × 0.5 column volumes of elution buffer [50 mM Tris-HCl (pH 8), 200 mM NaCl, and 500 mM imidazole]. Elutions containing protein were collected and dialyzed against 3 × 1 L in buffer [50 mM Tris-HCl (pH 8) and 200 mM NaCl]. The protein was stored at −80 °C.

Isolation of Membrane Fractions Containing WcfS. WcfS was isolated as described above with a few minor changes. After sonication, lysed cells were homogenized on ice and centrifuged at 856*g* for 25 min. The supernatant was spun at 150000*g* and 4 °C for 75 min. The pellet, containing membrane components, was homogenized in 3 mL of lysis buffer and stored at −80 °C. The total protein concentration was 4.6 mg/mL, as determined by the Bradford assay using BSA as a standard.

Detection of Recombinant Proteins. Purified protein was subjected to sodium dodecyl sulfate−polyacrylamide gel electrophoresis (SDS−PAGE) (10%) analysis for molecular weight confirmation, and protein was detected by staining gels with Coomassie R-250. Protein was also transferred to nitrocellulose for Western blot analysis. Nitrocellulose was stained with PonceauS to visualize all protein present. Nitrocellulose was then washed and blocked for at least 4 h in 5% milk in PBS containing 0.05% Tween 20 (PBS-T) and then washed for 3 × 15 min with PBS-T. Nitrocellulose-containing proteins were incubated overnight with a 1:3000 dilution of mouse anti-His antibody (GE Heathcare) or 1:10000 dilution of anti-T7 antibody linked to alkaline phosphatase (Pierce) diluted in PBS-T. Unbound antibody was removed with 3 × 15 min PBS-T washes. Blots were then incubated with a 1:10000 dilution of anti-mouse antibody linked to alkaline phosphatase (Pierce) for 4 h or overnight and then washed as described above. All proteins were detected using NBT/BCIP (Pierce).

Cross-Linking Studies of WcfR. WcfR was mixed with BS^3 cross-linking reagent (Pierce) as follows: 17 μM WcfR, 25 mM bicine (pH 8.5), 150 mM NaCl, and 435 μM BS^3. Aliquots (15 μL) were removed from the solution at 0.5, 1, 4, and 8 min and mixed with 10 μL of 1.5 M Tris-HCl to quench the reaction. Samples were then loaded onto a 5% SDS−PAGE gel and analyzed by gelcode blue staining (Pierce).

Dynamic Light Scattering Studies of WcfR. WcfR samples were dialyzed overnight in 25 mM bicine (pH 8.5) and 150 mM NaCl. Small particulates were removed by centrifugation. Samples were then analyzed using standard methods for dynamic light scattering on a DynaPro NanoStar Light Scatterer at the MIT bioinstrumentation facility.

Analytical Separation of UDP-Sugars Using HPLC. The sugar standards, UDP-GlcNAc, UDP-AADGal, and UDP-4-keto sugar (ranging from 2.8 to 4.0 nmol), were separated by HPLC with an aminopropyl-linked silane column (Agilent Zorbax NH_2, 5 μm, 4.6 mm × 250 mm) and column guard. Separations were performed for sugar analysis using 150 mM ammonium acetate at a flow rate of 2 mL/min at pH 4.5. The uridine ring of the sugar was detected by monitoring the absorbance at 260 nm with a 4 nm bandwidth.

Preparative Separation of UDP-Sugars. Preparative scale isolations of UDP-sugars were performed as described above with slight modifications. Preparative isolations used an isocratic method with 25−50 mM ammonium acetate (pH 4.5) (flow rate of 1 mL/min). UDP-sugars that were isolated using this method were dried overnight, and the remaining acetate and other contaminants were removed by passing the sugars over a preparative scale C18 column (Varian 250 mm × 21.2 mm column) using a 25 mM ammonium bicarbonate mobile phase (flow rate of 4 mL/min).

Analytical Separations by Capillary Electrophoresis. Samples were filtered through spin concentrators (Millipore Centrifugal Filter Units) spun at 19745*g* for 15 min and diluted (1:1) with water. A 40 μL sample was loaded into 0.5 mL CE vials, and the vials were loaded onto the system. The bare silica capillary (polymicro, 49 μm × 45 cm) was washed with running buffer [100 mM borate (pH 9.15)] for 3 min before each analysis. Samples were introduced by pressure injection for 10 s at 0.5 psi, and the separation was performed at 15 kV. Reaction and standard components were monitored at 260 nm.

TLC Analysis of Bactoprenyl-Linked Reaction Components. Reaction mixtures contained 1.4 nmol of NA-B-P synthesized as described previously[26] except using ammonium form isopentenyl diphosphate, or 5 nmol of undecaprenol purchased from ARC, 20 μL of membrane fraction (92 μg of total protein) containing WcfS, 1.5 nmol of UDP-[^{3}H]AADGal (79 dpm/pmol), 50 mM TrisOAc (pH 8.0), 1% Triton X-100, 10 mM $MgCl_2$, 1 mM ATP, and 20 μL of a membrane fraction containing *Streptococcus mutans* diacylglycerol kinase (transfers phosphate from ATP to undecaprenol providing in situ undecaprenyl phosphate[27]) in a total volume of 200 μL. Reaction mixtures were incubated at room temperature for 1 h, and then 50 μL was quenched in 800 μL of a 2:1 $CHCl_3$/MeOH mixture. The organic layer was washed with 3 × 200 μL of pure solvent upper phase (PSUP, 4% KCl in a 1:1 methanol/water mixture). The organic layer was dried under a stream of air and redissolved in 200 μL of DMSO. Separately, the organic and aqueous layers were diluted in 4.7 mL of ECOLITE scintillation fluid and were counted on a Perkin-Elmer Tricarb scintillation counter. The percent turnover was calculated from the amount of tritium in each layer. Each reaction was performed in duplicate, including controls that did not contain WcfS. The remaining reaction mixture was extracted as described above, and the organic layer was dried on a vacuum concentrator. The residue was dissolved in 50 μL of *n*-propanol and then spotted on Whatman K6F TLC plates. Plates were resolved in a 73:53:11 $CHCl_3$/MeOH/0.1 M sodium borate mixture over 50 mm. The labeled product was then analyzed on a Bioscan AR-2000 radio-TLC imaging scanner. UDP-[^{3}H]-AADGal was also spotted and analyzed via identical methods. In addition, the origin and solvent front of the TLC plates were also spotted to ensure appropriate calibration of the imaging scanner position.

Reverse Phase HPLC Analysis of Bactoprenyl-Linked Reaction Components. Reverse phase (RP) isocratic HPLC on bactoprenol-linked materials was performed on a C18 column (Agilent Eclipse XDB-C18, 5 μm, 4.6 mm × 150 mm) in a 50% *n*-propanol/50% ammonium bicarbonate (25 mM) mixture. Products were purified using an isocratic method with a 75% *n*-propanol/25% ammonium bicarbonate (25 mM) mixture on a C18 Varian 250 mm × 21.2 mm column (flow rate of 4.0 mL/min).

Enzymatic Reactions of WcfR. WcfR function was analyzed with 2.6 nmol of standard UDP-4-keto sugar produced as described previously[15] with 15 mM L-glutamate and 100 μM pyridoxal 5′-phosphate (PLP) in 50 mM Tris-acetate (pH 8) and 50 mM NaCl and analyzed using CE. To synthesize UDP-AADGal, a two-step coupled reaction of WcfR and the characterized *Campylobacter jejuni* dehydratase, PglF, was used.[15] The UDP-4-keto sugar was produced using the PglF conditions previously described by Olivier et al. with 0.64 mg of $PglF_{130}$ enzyme in a 1 mL solution. After 10 h, 0.16 mg of purified WcfR was added to the reaction solution along with 15 mM L-glutamate and 100 μM pyridoxal 5′-phosphate (PLP); the mixture was incubated for 4−6 h at 28 °C. Reaction mixtures with PglF and WcfR were analyzed by CE and then isolated and purified using HPLC. After vacuum concentration, the UDP-AADGal sugar product was quantified spectrophotometrically.

Synthesis of UDP-[^{3}H]AADGal. UDP-[^{3}H]AADGal was synthesized using the two-step reaction described above. A 100 μL reaction mixture with 10 μL of UDP-[^{3}H]GlcNAc (8752 dpm/pmol), 0.33 μM UDP-GlcNAc, 25 μM NAD^+, 0.1% Triton X-100, and 160 ng of PglF was incubated for 6 h, after which an additional 160 ng of PglF was added, and the mixture was incubated at room temperature overnight. PLP (100 μM) and L-glutamate (15 mM) (final concentrations) were added along with 200 ng of WcfR, and the mixture was incubated for 4 h at room temperature. After incubation, the UDP-[^{3}H]-AADGal was isolated using HPLC as described above.

Enzymatic Reactions of WcfS. The NA-B-PP-AADGal was prepared by adding 5 μL of the WcfS membrane fraction (23 μg of total protein) to a 200 μL solution containing 0.1 nmol of NA-B-P *cis*-6 or *cis*-7, 19.6 nmol of UDP-AADGal, 1% hydrogenated Trition X-100, 10 mM $MgCl_2$, 0.5% DMSO, and 50 mM Tris-HCl. The reaction mixture was incubated at room temperature for 30 min and was analyzed using the RP-HPLC method described above. Two negative controls, one containing no WcfS and the other containing no UDP-AADGal, were prepared for comparison.

Coupling of WcfR and WcfS. A 200 μL reaction mixture was prepared as described above with the addition of 15 mM L-glutamate, 100 μM PLP, and 26 nmol of UDP-4-keto sugar in place of UDP-AADGal. To test the coupling of WcfR, WcfS, and PglF, a 200 μL reaction mixture was prepared as described for the WcfR−WcfS reaction in addition to 25 μM NAD^+ and 33 nmol of UDP-GlcNAc. Controls in the absence of sugar were also prepared. The coupled reactions and controls were incubated for 30 min at room temperature and analyzed by HPLC.

RESULTS

Isolation and Biophysical Characterization of WcfR. The reported structure of CPSA includes a rare α-linked acetamido-4-amino-6-deoxygalactopyranose (AADGal). The biosynthesis of a nucleotide-linked AADGal sugar (Scheme 1) has not been previously reported. However, two similar sugars, bacillosamine and 6-deoxy-4-amino-2-acetamido-L-altrose [AltNac (Figure 2)], have been reported as products of *C. jejuni* aminotransferases PglE and PseC, respectively.[15,17] The CPSA biosynthesis gene locus in *B. fragilis* includes a proposed aminotransferase, WcfR, which is 48% similar to PglE, and

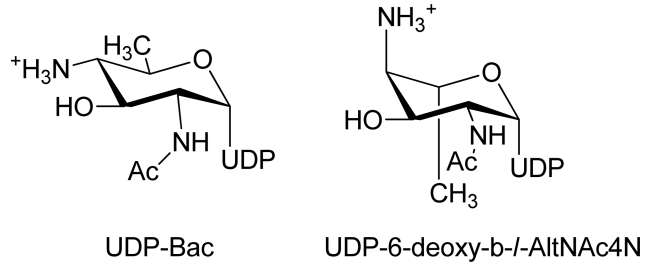

UDP-Bac UDP-6-deoxy-b-/-AltNAc4N

Figure 2. Previously characterized UDP-linked 6-deoxy-4-amino sugars.

dx.doi.org/10.1021/bi400126w | *Biochemistry* 2013, 52, 1939−1949

PseC. The relatively low level of sequence similarity to well-characterized aminotransferases prompted us to isolate WcfR for biochemical characterization. The gene encoding the predicted aminotransferase was amplified from *B. fragilis* genomic DNA and incorporated into a pET-24a vector. The protein was expressed in *E. coli* BL-21(DE3) RIL cells and purified by Ni-NTA affinity chromatography. The presence of the recombinant protein was confirmed by Western Blot analysis (Figure 1 of the Supporting Information). More than 16 mg of protein was isolated per liter of cell culture. Dynamic light scattering studies of the protein suggested that it was a monodispersed dimer consistent with similar proteins previously characterized (Figure 2 of the Supporting Information).[28] Cross-linking studies using the water-soluble cross-linker BS^3 confirmed the presence of the dimer in solution (Figure 3 of the Supporting Information).

WcfR Catalyzes the Formation of UDP-AADGal from a UDP-4-Keto Sugar. WcfR amino acid sequence analysis suggested that it was a member of the aspartate aminotransferase (AAT) superfamily that utilizes a pyridoxal 5′-phosphate (PLP) as an electron sink for transamination reactions. However, some AAT family members play a role in elimination, decarboxylation, and racemization reactions.[15,17] To test the proposed function of the recombinant WcfR, a UDP-4-keto sugar (Scheme 1) was required. Efforts to isolate *B. fragilis* dehydratase UngD2, previously reported through genetic studies[12] to produce the WcfR substrate, were unsuccessful. *C. jejuni* protein PglF catalyzes the formation of a UDP-4-keto sugar with the appropriate stereochemistry at position 5″ from UDP-GlcNAc. To bypass the need of the *B. fragilis* enzyme and to determine if we could replace it with an enzyme from another organism, PglF was isolated and utilized to produce the UDP-4-keto sugar as described previously.[15] Purified WcfR was incubated with the UDP-4-keto sugar, PLP, and L-glutamate. Product formation was then analyzed by capillary electrophoresis (CE) (Figure 3). The UDP-4-keto

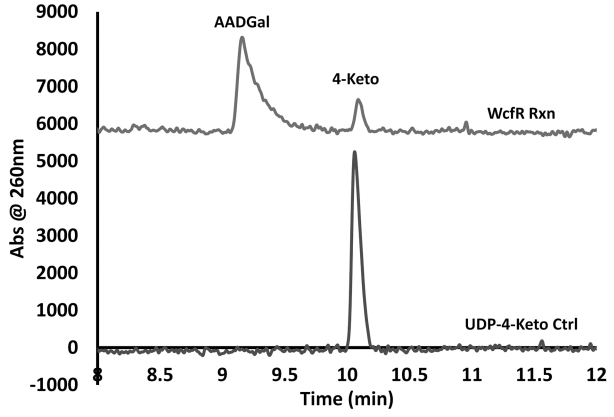

Figure 3. Capillary electrophoresis analysis confirms the function of WcfR. CE analysis of the 0.33 mM UDP-4-keto sugar standard isolated from PglF and a WcfR reaction with 0.33 mM UDP-4-keto sugar in the presence of 0.08 mg of WcfR, PLP, and L-glutamate.

sugar was >90% consumed by WcfR to give a new peak with less electrophoretic mobility, which was consistent with the addition of an amino group. These results suggest that WcfR is the aminotransferase required for the biosynthesis of the AADGal sugar in CPSA.

Amine Resin-Based Isolation of UDP-Linked Sugars. Identifying the location of the incorporated amine in the UDP-AADGal sugar required a robust isolation method. A variety of methods are available for HPLC separation of UDP-sugars, including reverse phase (RP) on C18 with ion-pairing agents like triethylammonium bicarbonate (TEAB) and RP coupled to ion exchange methods using phosphate buffers.[15,29−34] However, in our hands, we were unable to separate similar sugars using the TEAB methods, and for further characterization, we were interested in utilizing a volatile buffer system rather than phosphate. A column consisting of an aminopropylsilane provided reproducible HPLC separations that could be easily controlled by pH or ammonium acetate buffer concentration. Of particular interest was the large difference in retention between the UDP-4-keto sugar and UDP-AADGal as shown in Figure 4. Note that the chromatogram shown in

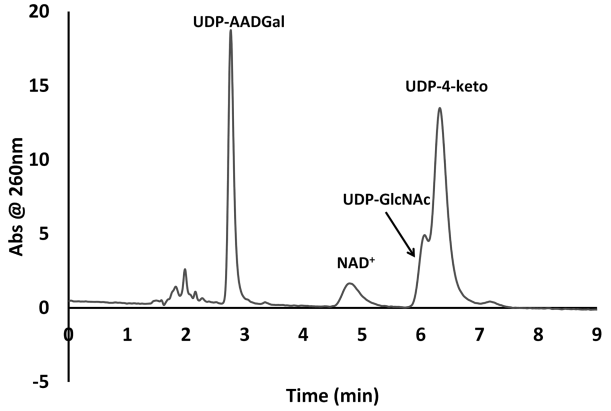

Figure 4. HPLC isolation of UDP-linked sugars on aminopropyl silane resin. (a) HPLC analysis of the PlgF−WcfR coupled reaction with 0.33 mM UDP-GlcNAc with 0.1 mg of PglF and 0.08 mg of WcfR in the presence of NAD^+, PLP, and L-glutamate. Run with 150 mM ammonium acetate at a flow rate of 2 mL/min at pH 4.5.

Figure 4 is the midpoint of a PglF−WcfR coupled reaction described below. The use of the aminopropylsilane column provided excellent separation of the reaction components and may provide a novel method for the separation of other similar UDP-sugars.

Characterization of UDP-AADGal. The unusual stereoconfiguration and identity of the UDP-AADGal isolated by HPLC were determined through a series of spectroscopic studies. The expected molecular weight of UDP-AADGal (589.1 amu) was confirmed by negative ion mode ESI-MS as shown in Figure 5, where only the −1 ion was detected. High-resolution MS analysis further demonstrated the expected molecular weight of the product and the insertion of an amine in the sugar structure (Figure 4 of the Supporting Information). Proton-decoupled ^{31}P NMR (Figure 5 of the Supporting Information) analysis suggested the presence of the linking diphosphate moiety, and J coupling values (Table 1) of the clear phosphorus doublets were consistent with previously characterized UDP-sugars.[15,17,35] Analysis by one-dimensional ^1H NMR (Figure 5) was used for structural characterization with two-dimensional correlation spectroscopy [COSY (Figure 6 of the Supporting Information)] to independently assign the spectrum. The chemical shifts and COSY correlations are listed in Table 1 for the entire UDP-sugar. Using the COSY spectrum, we were able to assign each peak of the pyranose ring and found the chemical shifts to be consistent with similar

dx.doi.org/10.1021/bi400126w | *Biochemistry* 2013, 52, 1939−1949

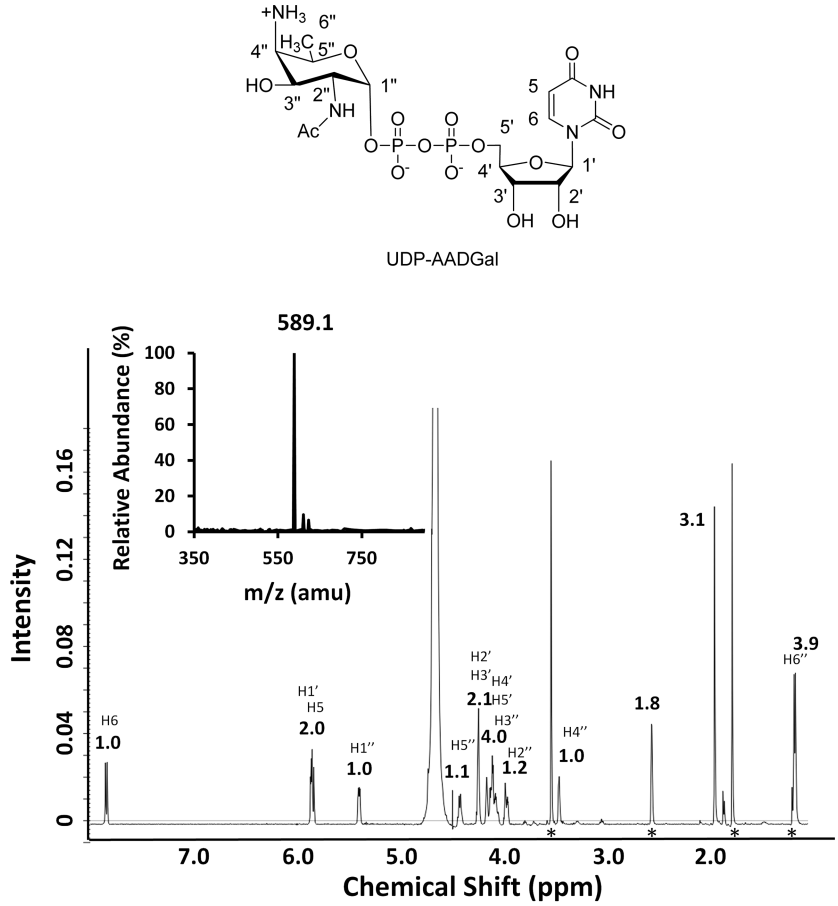

Figure 5. Characterization of the UDP-AADGal product of WcfR. ^{1}H NMR including carbon designations, assignments, and integrals of each peak. The inset is the (−)ESI-MS spectrum showing a single peak with an expected molecular weight of 589.1. Asterisks denote contaminants.

Table 1. One- and Two-Dimensional NMR of UDP-AADGal[a]

moiety	δ_H (ppm)	J (Hz)	COSY correlation	TROESY correlation	TROESY integral
uracil					
H5	5.85	8.3	7.84 (H6)		
H6	7.84	8.1		4.24 (H2′/3′), 5.84 (H5)	−5.26, −3.76
ribose					
H1′	5.86	4.2	4.26 (H2′)	4.24 (H2′)	−2.08
H2′	4.26				
H3′	4.26		4.17 (H4′)		
H4′	4.17			5.87 (H1′)	−0.58
H5′a	4.08				
H5′b	4.13				
diphosphate					
Pa	−10.8	20.7			
Pb	−12.7	20.1			
pyranose					
H1″	5.40	3.5, 7.5	3.97 (H2″)	3.97 (H2″)	−6.02
H2″	3.97		4.11 (H3″)	4.13 (H3″)	−0.84
H3″	4.11		3.48 (H4″)	3.47 (H4″)	−7.12
H4″	3.48		4.43 (H5″)	1.18 (H6″)	−1.46
H5″	4.43		1.19 (H6″)	3.47 (H4″), 4.11 (H3″)	−8.12, −9.16
H6″	1.19	6.9		4.43 (H5″)	−6.83
acetyl	2.06				

[a]COSY and TROESY correlations are provided for each unique peak. T-ROESY integrals are provided as demonstrations of cross-peak magnitude. T-ROESY integrals are negative because of the phase dependence of the experiment.

sugars from other bacterial systems (Table 2 of the Supporting Information).[15,17,35] However, the COSY and ^{1}H NMR spectra could not provide stereochemical information about the product.

dx.doi.org/10.1021/bi400126w | *Biochemistry* 2013, 52, 1939−1949

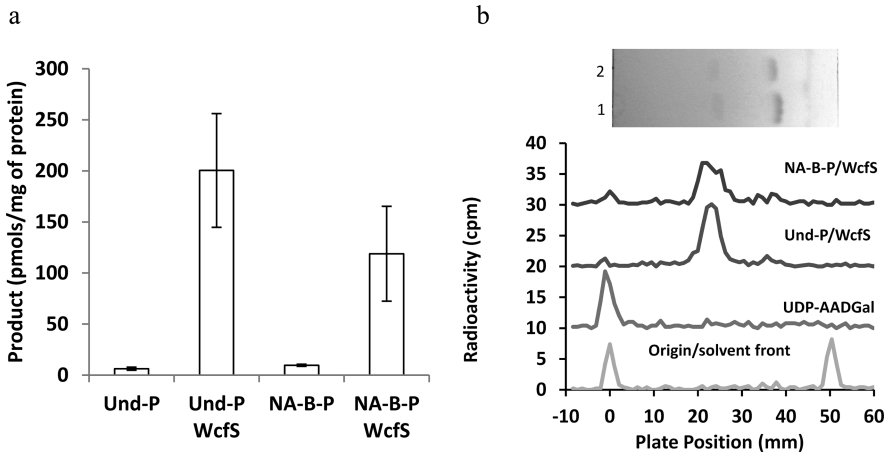

Figure 6. WcfS utilization of UDP-AADGal, undecaprenol, and NA-B-P *cis*-7. (a) Reaction mixtures containing 5 nmol of UndOH or 1.4 nmol of NA-B-P *cis*-7 were mixed with 92 μg of total protein WcfS membrane fraction and 1.5 nmol of UDP-[^{3}H]AADGal. A 20 μL aliquot of product was extracted into $CHCl_3$ and washed with Pure Solvent Upper phase. Organic and aqueous phases were counted on a scintillation counter. The percent incorporation was calculated by the amount of radiolabel in the organic layer relative to the total and converted to picomoles of product per microgram of total protein in the reaction mixture. (b) TLC analysis of the dried remaining reaction from organic extractions on the TLC plate scanner: (origin/solvent front) origin and solvent front markers for calibration, (UDP-AADGal) sugar alone, (Und-P/WcfS) WcfS reaction mixture with UndOH, and (NA-B-P/WcfS) WcfS reaction mixture with an analogue. The TLC plate contained NA-B-P *cis*-7 (lane 1) and NA-B-P *cis*-6 (lane 2) large scale reaction product with WcfS and UDP-AADGal. The TLC plate is contrast-enhanced to aid visualization.

Stereoconfiguration of UDP-AADGal. To characterize the stereochemical configuration of UDP-AADGal, we used phase-dependent transverse rotating-frame Overhauser enhancement spectroscopy [T-ROESY (Figure 7 of the Supporting Information)]. This NMR technique allowed the detection of clear through-space interactions and the magnitude of those interactions between each of the pyranose ring protons (Table 1). We observed a relatively strong interaction between H1″ and H2″ (Figure 5) as determined by the integral magnitude (Table 1). However, the magnitude of the integral for a cross-peak between H2″ and H3″ was very weak, suggesting these were on opposite sides of the sugar. There was a strong correlation (>5 integral units) between H3″ and H4″, H4″ and H5″, and H5″ and H3″, suggesting that all of these protons were on the same side of the pyranose ring. There was a relatively weak through-space interaction associated with the H4″−H6″ cross-peak, suggesting some proximity between the C6″ methyl group and the equatorial H4″. As expected, there was also a strong correlation between the H5″ and the C6″ methyl protons. Altogether, these results strongly support the proposed stereoconfiguration of the novel UDP-AADGal sugar, which is identical to that of the unlinked sugar previously described in CPSA.[36]

Similarity of WcfS to a Known Initiating Hexose-1-phosphate Transferase. Initiating hexose-1-phosphate transferases link phospho sugars from UDP-linked sugars to bactoprenyl phosphate (B-P) scaffolds. The similarity of the AADGal sugar to the characterized di-N-Ac-bacillosamine of *C. jejuni* prompted us to assume that the AADGal was the first sugar to be incorporated into the bactoprenyl scaffold in CPSA biosynthesis (Scheme 1).[37−39] Of the four proposed glycosyltransferases present in the CPSA biosynthesis gene locus, one gene was similar to the initiating hexose-1-phosphate transferase from *C. jejuni*, PglC. The protein encoded by the *wcfS* gene was 41% identical and 60% similar to the *C. jejuni* initiating hexose-1-phosphate transferase, suggesting that the WcfS protein may transfer the AADGal sugar phosphate to bactoprenyl phosphate.

WcfS Expression. To test the function of WcfS, the gene encoding the predicted initiating hexose-1-phosphate transferase was amplified by PCR and incorporated into a pET-24a vector that encoded a C-terminal hexahistidine tag. The plasmid encoding WcfS was transformed into BL-21(DE3) RIL cells, and protein was expressed using autoinduction. WcfS was predicted to contain one transmembrane domain by the TMHMM prediction software (Figure 8 of the Supporting Information).[40] WcfS could be functionally isolated in the membranes of the *E. coli* expression cells. Western blot analysis was used to confirm the presence of the recombinant protein in the membrane fraction (Figure 1 of the Supporting Information). It is important to note that the WcfS protein was ligated into a pET-24a vector that did not include an N-terminal T7 tag coding sequence. As expected, the WcfS protein was not detected using an anti-T7 antibody but was detected using the anti-His antibody.

WcfS Catalyzes the Transfer of [^{3}H]AADGal to Bactoprenyl Phosphate. WcfS was thought to link phospho-AADGal to bactoprenyl phosphate. To test the function of WcfS, we first synthesized a radiolabeled UDP-[^{3}H]AADGal from UDP-[^{3}H]GlcNAc, as described above with unlabeled material. The product of this reaction was characterized by RP-HPLC analysis and comparison with an authentic unlabeled product. The specific activity was calculated from the UV absorbance of the uridine ring at 260 nm and the tritium count of the purified UDP-[^{3}H]AADGal. Using the method of Hartley, Larkin, and Imperiali,[27] undecaprenyl phosphate was produced from commercially available plant undecaprenol and *S. mutans* diacylglycerol kinase, which has been shown to monophosphorylate undecaprenol. The reaction solution was then mixed with UDP-[^{3}H]AADGal and the WcfS-containing membrane fraction (Scheme 1). The organic soluble undecaprenyl-linked product was next isolated by organic−aqueous extraction. We found, as shown in Figure 6a, that the presumed initiating hexose-1-phosphate transferase, WcfS, could transfer the water-soluble [^{3}H]AADGal to the organic soluble undecaprenol.

dx.doi.org/10.1021/bi400126w | *Biochemistry* 2013, 52, 1939−1949

Reaction of Bactoprenyl Analogues in WcfS-Catalyzed Reactions. Previously, our group has described the use of a *p*-nitroaniline bactoprenyl phosphate [NA-B-P (Figure 7)]

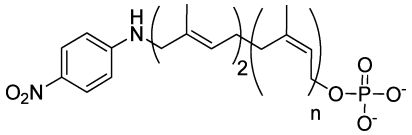

NA-B-P *cis*-6 *n*=6
NA-B-P *cis*-7 *n*=7

Figure 7. NA-B-P analogue. *cis*-6 and *cis*-7 denote analogues with six and seven *z*-configuration isoprenes, respectively.

analogue with the WcfS homologue PglC from *C. jejuni*.[26] This analogue provided significant advantages over reactions with undecaprenol in that it could be readily detected by HPLC and TLC analysis, which would allow for simple isolation of very small quantities of the product without the use of expensive radiolabels. To initially test the activity of the analogue, the WcfS membrane fraction and UDP-[^{3}H]AADGal were mixed with NA-B-P *cis*-7. By extraction analysis, as described above, the transfer of tritium to the organic soluble NA-B-P was observed, as shown in Figure 6a. TLC analysis of the NA-B-P and undecaprenol reactions revealed a new radioactive material with similar retention factors formed in both reactions, as shown in Figure 6b. The radiolabel was incorporated into a product with mobility drastically increased from that of the UDP-[^{3}H]AADGal substrate. Separately, in larger-scale reaction mixtures, we observed a light yellow spot with the same retention factor observed with the radioactive samples. These results strongly suggested that WcfS did catalyze the transfer of phospho-AADGal to the analogue. Control reactions with WcfS replaced with only the kinase membrane fraction did not result in an altered mobility of the reactants.

HPLC Isolation of Bactoprenyl-Linked AADGal. Utilizing undecaprenol as a substrate for initiating hexose-1-phosphate transferases makes it difficult to isolate the modified product as there is no easily distinguishable chromophore associated with the molecule. However, the *p*-nitroaniline moiety on NA-B-P is easily distinguishable spectrophotometrically. We took advantage of this property of the analogue to test the activity of NA-B-P of different lengths (Figure 7) with WcfS. Reaction mixtures were prepared with unlabeled UDP-AADGal in excess of NA-B-P *cis*-6 or *cis*-7.[26] Product retention times were clearly distinguishable by RP-HPLC in a 50% *n*-PrOH/ammonium bicarbonate mixture, and there was a decrease in the level of retention with the increased polarity of the phospho-AADGal, as shown in panels a and b of Figure 8. We found that NA-B-Ps with both six and seven *cis* isoprene additions were substrates for WcfS. However, the turnover for the NA-B-P *cis*-7 (78%) isoprenoid was slightly lower than with the *cis*-6 (~90%) isoprenoid. These results were consistent with previous studies by the Walker group with multiple-length isoprenes and are presumably due to the increase in the level of micelle formation with the longer chain isoprenoids.[41] The product was isolated from the NA-B-P *cis*-6 reaction mixture, and the identity of the new product was confirmed by high-resolution MS analysis (Figure 9 of the Supporting Information).

PglF, WcfR, and WcfS Can Be Coupled for a Single-Pot Synthesis of Bactoprenyl Diphosphate-AADGal. A major advantage of the use of enzymes in the biosynthesis of complex

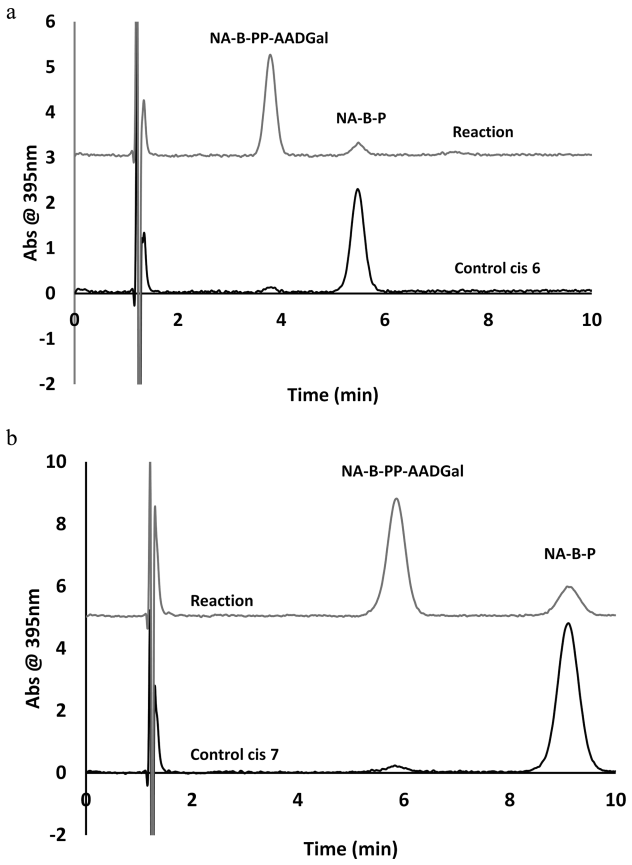

Figure 8. WcfS utilizes both *cis*-6 and *cis*-7 NA-B-P. (a) HPLC analysis of a control of 23 μg of the total protein WcfS membrane fraction in the presence of 20 μM NA-BP and no UDP-linked sugar. The reaction mixture contained the same amount of protein and analogue with 0.14 mM UDP-AADGal sugar. (b) Analysis of a reaction mixture identical to that described for panel a except with NA-B-P *cis*-7.

oligosaccharides is the selectivity of these proteins for specific substrates. We were interested in whether we could take advantage of this to biosynthesize the bactoprenyl diphosphate-linked monosaccharide in a single-pot reaction. First, PglF and WcfR were tested to determine if they could be readily coupled to give UDP-AADGal without isolation of the UDP-4-keto sugar. The results from the two-step reaction showed excellent turnover to the expected UDP-AADGal product. Figure 4 shows an intermediate timed reaction in which HPLC peaks are observed for UDP-GlcNAc, UDP-4-keto sugar, and UDP-AADGal. Reaction mixtures containing WcfS, WcfR, NA-B-P *cis*-7, and the UDP-4-keto sugar were also prepared. We found that there was full conversion to the monosaccharide product in this reaction, as shown in Figure 9a. Next, reaction mixtures containing WcfS, WcfR, and PglF with no sugar substrate or with UDP-GlcNAc were prepared. In the presence of all three proteins, substrates, and cofactors with UDP-GlcNAc, conversion to bactoprenyl diphosphate-linked product was observed (Figure 9b). These results demonstrate that all of the enzymes in this system can be coupled for the formation of the first CPSA bactoprenyl-linked sugar in a single-pot reaction.

DISCUSSION

In this report, we have taken the first critical step in the in vitro assembly of CPSA, a complex sugar polymer that has been shown to have therapeutic potential for inflammatory bowel

dx.doi.org/10.1021/bi400126w | *Biochemistry* 2013, 52, 1939−1949

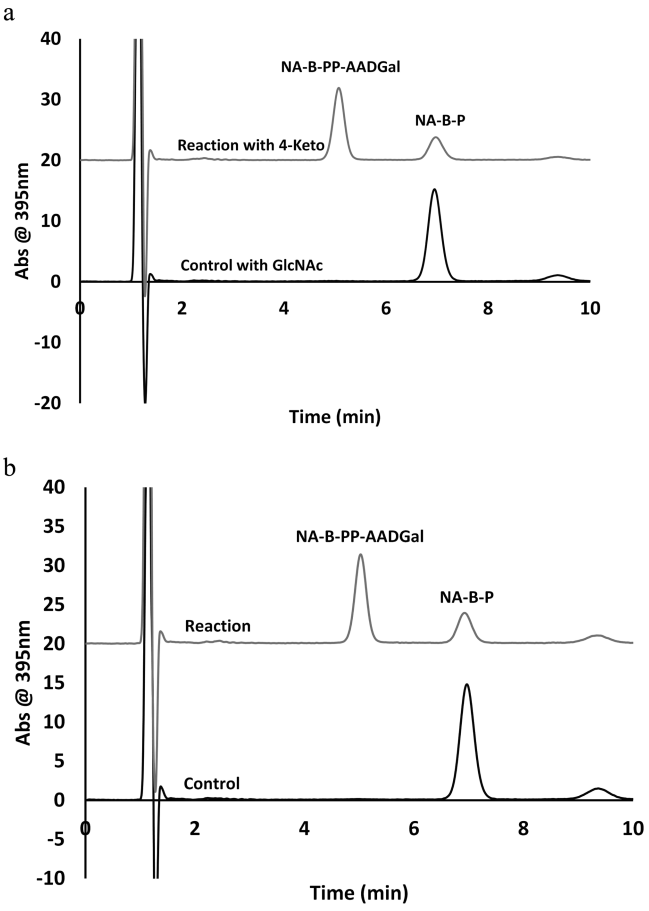

Figure 9. Single-pot biosynthesis of NA-B-PP-AADGal. (a) Analysis in a 1:1 PrOH/ammounium bicarbonate mixture on a C18 column of a reaction mixture containing 0.08 mg of WcfR and 23 μg of the total protein WcfS membrane fraction in the presence of 20 μM NA-BP, all necessary cofactors, and 0.33 mM UDP-GlcNAc (reaction with GlcNAc) or 0.26 mM UDP-4-keto sugar (reaction with 4-keto). (b) HPLC analysis in a 1:1 PrOH/ammounium bicarbonate mixture on a C18 column of a reaction mixture with 0.1 mg of PlgF, 0.08 mg of WcfR, and 5 μL of the WcfS membrane fraction in the presence of 20 μM NA-BP, all necessary cofactors, and UDP-GlcNAc (Reaction) or no sugar (Control).

disease as well as multiple sclerosis.[3,5] We have shown that the AADGal sugar can be readily formed using a combination of enzymes from *C. jejuni* and the native organism *B. fragilis*. We have also demonstrated the role of the initiating hexose-1-phosphate transferase, WcfS, which catalyzes the addition of AADGal to bactoprenol. There are three additional glycosyltransferase genes associated with the *B. fragilis* CPSA biosynthesis locus, *wcfN*, *wcfP*, and *wcfQ*. Here we have for the first time used a bactoprenyl phosphate probe to interrogate the first enzyme in this pathway and will be able to utilize the product from these reactions to readily identify the role of the remaining glycosyltransferases.

The AADGal stereochemistry has been reported in the native CPSA polysaccharide,[36] and we have clearly demonstrated that this sugar can be synthesized with WcfR and transferred to bactoprenyl phosphate by WcfS. However, it is possible that these enzymes could also utilize the previously characterized bacillosamine and L-AltNAc 4-amino sugars (Figure 2). It would be of great interest to determine the preferred substrate stereochemistry of the WcfR and WcfS proteins. In addition, the dehydratase responsible for biosynthesizing the substrate for WcfR has not been previously isolated. Work by the Comstock group has suggested that the dehydratase is encoded by the *ungD2* gene.[12] However, in our hands, we have not been able to demonstrate this function from the protein encoded by the *ungD2* gene. The biochemical role of this gene is of great importance and will be the subject of future work by our group.

The lack of a dehydratase in the CPSA biosynthesis locus required us to use the previously characterized soluble PglF from *C. jejuni* to provide the substrate needed to test WcfR function. It was interesting that we observed coupling with the soluble PglF and WcfR, because coupling was observed with only full-length PlgF and aminotransferase PglE in the *C. jejuni* Pgl pathway.[15] Crucially, it was of considerable interest that enzymes coupled from different organisms provided a function that was not readily observed with the native proteins of the organism in vitro. We have also shown in this report that a single-pot synthesis can be utilized for the biosynthesis of the first bactoprenyl diphosphate-linked monosaccharide using PglF, WcfR, and WcfS. One of the ultimate goals of our work is to produce CPSA. In the fulfillment of that goal, it would be ideal if we could couple as many enzymes as possible for the biosynthesis of this complex polysaccharide.

The unusual stereochemistry of the UDP-AADGal sugar prompted concern about the identity of the sugar produced by WcfR. UDP-4-amino sugar biosynthesis, similar to that of AADGal, has been characterized in a number of systems.[15−17,35] Comparison of our NMR data and the data obtained for the previously characterized UDP-sugars (Table 2 of the Supporting Information) strongly suggests that the sugar synthesized in this work is UDP-AADGal. The similar UDP-bacillosamine [UDP-Bac (Figure 2)] differs only in the stereochemistry of the 4″-amino group. Remarkably, proton peaks in the sugar reported here were identical (within 0.1 ppm) to those of UDP-Bac, except the chemical shifts associated with H3″, H4″, and H5″ of the pyranose ring. H3″, H4″, and H5″ were all shifted downfield 0.29, 0.49, and 0.24 ppm, respectively, relative to UDP-Bac.[17] It is very important to note that the position at which the stereochemistry is flipped in UDP-AADGal had the largest chemical shift difference. In addition, the L-AltNAc sugar (Figure 2) has the same stereochemistry as our 4-amino sugar at position H4″ but differs at position H5″. Between these two sugars, we observe the most significant chemical shift differences in H4″ and H5″ with values of 0.17 and 0.32 ppm, respectively. The largest shift difference again was between the UDP-AADGal and UDP-AltNAc sugar at the position that corresponded to the difference in stereochemistry. In addition to the phase-dependent T-ROESY results described above, the consistency with the previously characterized sugars strongly suggests the correct assignment of stereochemistry in this report. Interestingly, there is one report about the biosynthesis of an AADGal type of sugar.[35] However, later analysis of the activity of the same biosynthetic protein responsible for this sugar suggested that it actually had L-AltNAc stereochemistry.[17] In addition, the authors of the former report note a strong NOE between H1″ and H5″ of the pyranose ring consistent with the L-AltNAc 4-amino sugar stereochemistry.

The CSPA tetrasaccharide repeating unit has been characterized.[36] It has been suggested that AADGal was the initial sugar linked to a bactoprenyl membrane scaffold in a Wzy-dependent pathway for the biosynthesis of the sugar polymer.[12] The *wcfR* and *wcfS* genes were proposed to encode

dx.doi.org/10.1021/bi400126w | *Biochemistry* 2013, 52, 1939−1949

an aminotransferase and initiating hexose-1-phosphate transferase involved in linking phospho-AADGal to bactoprenyl phosphate.[13] In this work, we were able to demonstrate that WcfR exhibits aminotransferase activity and WcfS acts as an initiating hexose-1-phosphate transferase for the attachment of AADGal to an isoprenoid-linked membrane scaffold. In doing this, we developed a method of separating UDP-linked sugars and found that the aminotransferase WcfR produces a UDP-4-amino sugar with unreported stereochemistry. We were also able to couple WcfR and WcfS with a dehydratase from a different organism to produce the lipid-linked AADGal in a single-pot reaction. In addition, using our previously described bactoprenyl analogue, the progress of isoprenoid utilizing enzyme reactions could be readily monitored and products could be isolated. This work demonstrates a key step in a fully in vitro biosynthetic route to producing the potentially therapeutic CPSA from *B. fragilis*.

■ ASSOCIATED CONTENT

Supporting Information

Primer sequences used for cloning, NMR chemical shift comparisons with previously characterized sugars, Western blot and Ponceau analysis of expressed WcfR and WcfS, dynamic light scattering analysis, SDS−PAGE gel showing WcfR cross-linking, full COSY and T-ROESY spectra on UDP-AADGal, transmembrane domain prediction for WcfS, HR-MS of UDP-AADGal, and NA-B(*cis*-6)-PP-AADGal. This material is available free of charge via the Internet at http://pubs.acs.org.

■ AUTHOR INFORMATION

Corresponding Author

*Department of Chemistry, University of North Carolina at Charlotte, 9201 University City Blvd., Charlotte, NC 28223. E-mail: jerry.troutman@uncc.edu. Telephone: (704) 687-4494. Fax: (704) 687-0960.

Author Contributions

The manuscript was written through contributions of all authors. All authors have given approval to the final version of the manuscript.

Funding

This work was supported by National Institutes of Health AREA Grant R15GM100402 (J.M.T.).

Notes

The authors declare no competing financial interest.

■ ACKNOWLEDGMENTS

We thank Dr. Barbara Imperiali for PglF- and *S. mutans* kinase-expressing cells, Dr. Jian Liu for allowing us to use his MS system and for training, Dr. Michael Murphy and Richard Hardin for help with NMR data collection and processing, Dr. Brian Cooper for help with CE, Dave Hometchko for help with HPLC method development, Christina Martinez for synthesis of NAGPP, Sunita Sharma for early expressions of WcfS, Donovan Lujan for expression of WcfR, and Dr. Angelyn Larkin for critical reading of the manuscript and helpful suggestions.

■ ABBREVIATIONS

CPSA, capsular polysaccharide A; AADGal, acetamido-4-amino-6-deoxygalactopyranose; CE, capillary electrophoresis; HPLC, high-performance liquid chromatography; ESI-MS, electrospray ionization mass spectrometry; NMR, nuclear magnetic resonance; TLC, thin layer chromatography; NA−B-P, *p*-nitroaniline bactoprenol; WcfR, an aminotransferase; PlgF, a dehydratase; WcfS, an initiating hexose-1-phosphate transferase; FPP, farnesyl diphosphate; IPP, isopentenyl diphosphate; PCR, polymerase chain reaction; UDP, uridine diphosphate; GlcNAc, *N*-acetylglucosamine; GalNAc, *N*-acetylgalactosamine; PLP, pyridoxal 5′-phosphate; TEAB, triethylammonium bicarbonate; cef, cell envelope fraction; COSY, correlation spectroscopy; NOSEY, nuclear Overhauser effect spectroscopy; T-ROSEY, transverse rotating-frame Overhauser enhancement spectroscopy.

■ REFERENCES

(1) Tremaroli, V., and Backhed, F. (2012) Functional interactions between the gut microbiota and host metabolism. *Nature 489*, 242−249.

(2) Maynard, C. L., Elson, C. O., Hatton, R. D., and Weaver, C. T. (2012) Reciprocal interactions of the intestinal microbiota and immune system. *Nature 489*, 231−241.

(3) Surana, N. K., and Kasper, D. L. (2012) The yin yang of bacterial polysaccharides: Lessons learned from *B. fragilis* PSA. *Immunol. Rev. 245*, 13−26.

(4) Chung, H. C., and Kasper, D. L. (2010) Microbiota-stimulated immune mechanisms to maintain gut homeostasis. *Curr. Opin. Immunol. 22*, 455−460.

(5) Ochoa-Reparaz, J., Mielcarz, D. W., Wang, Y., Begum-Haque, S., Dasgupta, S., Kasper, D. L., and Kasper, L. H. (2010) A polysaccharide from the human commensal *Bacteroides fragilis* protects against CNS demyelinating disease. *Mucosal Immunol. 3*, 487−495.

(6) Cobb, B. A., Wang, Q., Tzianabos, A. O., and Kasper, D. L. (2004) Polysaccharide processing and presentation by the MHCII pathway. *Cell 117*, 677−687.

(7) Mazmanian, S. K., and Kasper, D. L. (2006) The love-hate relationship between bacterial polysaccharides and the host immune system. *Nat. Rev. Immunol. 6*, 849−858.

(8) Mazmanian, S. K., Liu, C. H., Tzianabos, A. O., and Kasper, D. L. (2005) An immunomodulatory molecule of symbiotic bacteria directs maturation of the host immune system. *Cell 122*, 107−118.

(9) Pragani, R., and Seeberger, P. H. (2011) Total synthesis of the *Bacteroides fragilis* zwitterionic polysaccharide A1 repeating unit. *J. Am. Chem. Soc. 133*, 102−107.

(10) Pragani, R., Stallforth, P., and Seeberger, P. H. (2010) De novo synthesis of a 2-acetamido-4-amino-2,4,6-trideoxy-D-galactose (AAT) building block for the preparation of a *Bacteroides fragilis* A1 polysaccharide fragment. *Org. Lett. 12*, 1624−1627.

(11) Kalka-Moll, W. M., Tzianabos, A. O., Wang, Y., Carey, V. J., Finberg, R. W., Onderdonk, A. B., and Kasper, D. L. (2000) Effect of molecular size on the ability of zwitterionic polysaccharides to stimulate cellular immunity. *J. Immunol. 164*, 719−724.

(12) Coyne, M. J., Chatzidaki-Livanis, M., Paoletti, L. C., and Comstock, L. E. (2008) Role of glycan synthesis in colonization of the mammalian gut by the bacterial symbiont *Bacteroides fragilis*. *Proc. Natl. Acad. Sci. U.S.A. 105*, 13099−13104.

(13) Coyne, M. J., Tzianabos, A. O., Mallory, B. C., Carey, V. J., Kasper, D. L., and Comstock, L. E. (2001) Polysaccharide biosynthesis locus required for virulence of *Bacteroides fragilis*. *Infect. Immun. 69*, 4342−4350.

(14) Comstock, L. E., Coyne, M. J., Tzianabos, A. O., Pantosti, A., Onderdonk, A. B., and Kasper, D. L. (1999) Analysis of a capsular polysaccharide biosynthesis locus of *Bacteroides fragilis*. *Infect. Immun. 67*, 3525−3532.

(15) Olivier, N. B., Chen, M. M., Behr, J. R., and Imperiali, B. (2006) In vitro biosynthesis of UDP-N,N′-diacetylbacillosamine by enzymes of the *Campylobacter jejuni* general protein glycosylation system. *Biochemistry 45*, 13659−13669.

(16) Creuzenet, C., and Lam, J. S. (2001) Topological and functional characterization of WbpM, an inner membrane UDP-GlcNAc C6

dehydratase essential for lipopolysaccharide biosynthesis in *Pseudomonas aeruginosa*. *Mol. Microbiol. 41*, 1295−1310.
(17) Schoenhofen, I. C., McNally, D. J., Vinogradov, E., Whitfield, D., Young, N. M., Dick, S., Wakarchuk, W. W., Brisson, J. R., and Logan, S. M. (2006) Functional characterization of dehydratase/aminotransferase pairs from *Helicobacter* and *Campylobacter*: Enzymes distinguishing the pseudaminic acid and bacillosamine biosynthetic pathways. *J. Biol. Chem. 281*, 723−732.
(18) Yother, J. (2011) Capsules of *Streptococcus pneumoniae* and other bacteria: Paradigms for polysaccharide biosynthesis and regulation. *Annu. Rev. Microbiol. 65*, 563−581.
(19) Woodward, R., Yi, W., Li, L., Zhao, G. H., Eguchi, H., Sridhar, P. R., Guo, H. J., Song, J. K., Motari, E., Cai, L., Kelleher, P., Liu, X. W., Han, W. Q., Zhang, W. P., Ding, Y., Li, M., and Wang, P. G. (2010) In vitro bacterial polysaccharide biosynthesis: Defining the functions of Wzy and Wzz. *Nat. Chem. Biol. 6*, 418−423.
(20) Han, W. Q., Wu, B. L., Li, L., Zhao, G. H., Woodward, R., Pettit, N., Cai, L., Thon, V., and Wang, P. G. (2012) Defining Function of Lipopolysaccharide O-antigen Ligase WaaL Using Chemoenzymatically Synthesized Substrates. *J. Biol. Chem. 287*, 5357−5365.
(21) Whitfield, C. (2006) Biosynthesis and assembly of capsular polysaccharides in *Escherichia coli*. *Annu. Rev. Biochem. 75*, 39−68.
(22) Whitfield, C., and Paiment, A. (2003) Biosynthesis and assembly of Group 1 capsular polysaccharides in *Escherichia coli* and related extracellular polysaccharides in other bacteria. *Carbohydr. Res. 338*, 2491−2502.
(23) Nielsen, P., and Krogh, A. (2005) Large-scale prokaryotic gene prediction and comparison to genome annotation. *Bioinformatics 21*, 4322−4329.
(24) Rodriguez-Ortega, M. J., Luque, I., Tarradas, C., and Barcena, J. A. (2008) Overcoming function annotation errors in the Gram-positive pathogen *Streptococcus suis* by a proteomics-driven approach. *BMC Genomics 9*, 588.
(25) Studier, F. W. (2005) Protein production by auto-induction in high density shaking cultures. *Protein Expression Purif. 41*, 207−234.
(26) Lujan, D. K., Stanziale, J. A., Mostafavi, A. Z., Sharma, S., and Troutman, J. M. (2012) Chemoenzymatic synthesis of an isoprenoid phosphate tool for the analysis of complex bacterial oligosaccharide biosynthesis. *Carbohydr. Res. 359*, 44−53.
(27) Hartley, M. D., Larkin, A., and Imperiali, B. (2008) Chemoenzymatic synthesis of polyprenyl phosphates. *Bioorg. Med. Chem. 16*, 5149−5156.
(28) Larkin, A., Olivier, N. B., and Imperiali, B. (2010) Structural Analysis of WbpE from *Pseudomonas aeruginosa* PAO1: A Nucleotide Sugar Aminotransferase Involved in O-Antigen Assembly. *Biochemistry 49*, 7227−7237.
(29) Carrey, E. A., Smolenski, R. T., Edbury, S. M., Laurence, A., Marinaki, A. M., Duley, J. A., Zhu, L., Goldsmith, D. J., and Simmonds, H. A. (2003) Origin and characteristics of an unusual pyridine nucleotide accumulating in erythrocytes: Positive correlation with degree of renal failure. *Clin. Chim. Acta 335*, 117−129.
(30) Cataldi, T. R., Campa, C., and De Benedetto, G. E. (2000) Carbohydrate analysis by high-performance anion-exchange chromatography with pulsed amperometric detection: The potential is still growing. *Fresenius' J. Anal. Chem. 368*, 739−758.
(31) Dorion, S., and Rivoal, J. (2003) Quantification of uridine 5′-diphosphate (UDP)-glucose by high-performance liquid chromatography and its application to a nonradioactive assay for nucleoside diphosphate kinase using UDP-glucose pyrophosphorylase as a coupling enzyme. *Anal. Biochem. 323*, 188−196.
(32) Pieslinger, A. M., Hoepflinger, M. C., and Tenhaken, R. (2009) Nonradioactive enzyme measurement by high-performance liquid chromatography of partially purified sugar-1-kinase (glucuronokinase) from pollen of *Lilium longiflorum*. *Anal. Biochem. 388*, 254−259.
(33) Tomiya, N., Ailor, E., Lawrence, S. M., Betenbaugh, M. J., and Lee, Y. C. (2001) Determination of nucleotides and sugar nucleotides involved in protein glycosylation by high-performance anion-exchange chromatography: Sugar nucleotide contents in cultured insect cells and mammalian cells. *Anal. Biochem. 293*, 129−137.
(34) Yang, T., and Bar-Peled, M. (2010) Identification of a novel UDP-sugar pyrophosphorylase with a broad substrate specificity in *Trypanosoma cruzi*. *Biochem. J. 429*, 533−543.
(35) Obhi, R. K., and Creuzenet, C. (2005) Biochemical characterization of the *Campylobacter jejuni* Cj1294, a novel UDP-4-keto-6-deoxy-GlcNAc aminotransferase that generates UDP-4-amino-4,6-dideoxy-GalNAc. *J. Biol. Chem. 280*, 20902−20908.
(36) Baumann, H., Tzianabos, A. O., Brisson, J. R., Kasper, D. L., and Jennings, H. J. (1992) Structural elucidation of two capsular polysaccharides from one strain of *Bacteroides fragilis* using high-resolution NMR spectroscopy. *Biochemistry 31*, 4081−4089.
(37) Glover, K. J., Weerapana, E., Chen, M. M., and Imperiali, B. (2006) Direct biochemical evidence for the utilization of UDP-bacillosamine by PglC, an essential glycosyl-1-phosphate transferase in the *Campylobacter jejuni* N-linked glycosylation pathway. *Biochemistry 45*, 5343−5350.
(38) Weerapana, E., Glover, K. J., Chen, M. M., and Imperiali, B. (2005) Investigating bacterial N-linked glycosylation: Synthesis and glycosyl acceptor activity of the undecaprenyl pyrophosphate-linked bacillosamine. *J. Am. Chem. Soc. 127*, 13766−13767.
(39) Glover, K. J., Weerapana, E., and Imperiali, B. (2005) In vitro assembly of the undecaprenylpyrophosphate-linked heptasaccharide for prokaryotic N-linked glycosylation. *Proc. Natl. Acad. Sci. U.S.A. 102*, 14255−14259.
(40) Krogh, A., Larsson, B., von Heijne, G., and Sonnhammer, E. L. (2001) Predicting transmembrane protein topology with a hidden Markov model: Application to complete genomes. *J. Mol. Biol. 305*, 567−580.
(41) Perlstein, D. L., Zhang, Y., Wang, T. S., Kahne, D. E., and Walker, S. (2007) The direction of glycan chain elongation by peptidoglycan glycosyltransferases. *J. Am. Chem. Soc. 129*, 12674−12675.